Incommensurate antiferromagnetism in the intermetallic superconductor $HoNi_2B_2C$

J. P. Hill, B. J. Sternlieb, and D. Gibbs
Department of Physics, Brookhaven National Laboratory, Upton, New York 11973

C. Detlefs, A. I. Goldman, C. Stassis, P. C. Canfield, and B. K. Cho
Ames Laboratory and Department of Physics and Astronomy, Iowa State University, Ames, Iowa 50011
(Received 25 August 1995)

We report high-resolution x-ray and neutron-scattering studies of the antiferromagnetism of the rare-earth superconductor, $HoNi_2B_2C$ ($T_C=8.5$ K). At low temperatures, $T<5$ K, the superconductivity coexists with a long-range ordered, commensurate Néel state. In the incommensurate antiferromagnetic state, 5 K$<T<$7 K, we find two phase coexistence between an a-axis modulation and a c-axis basal plane spiral-like structure. The c-axis structure is characterized by two wave vectors. Short-range ordered fluctuations of the commensurate phase, observed for $T>5$ K, are interpreted in terms of local strains.

Superconductivity arises from the Bose condensation of Cooper pairs; a pairing of electrons of opposite momenta and spin. Thus, in most superconductors even dilute concentrations of paramagnetic impurities suppress T_C, or destroy the superconductivity completely through spin-flip scattering.[1] Notable exceptions occur in compounds such as RMo_6S_8 and RRh_4B_4, where R is a magnetic rare-earth ion,[2] and the heavy-fermion superconductors,[3] all of which have evoked much interest. In these materials, magnetic ordering can coexist with superconductivity over a finite temperature range and the competition between these ground states has provided a wealth of data concerning the interaction between these two phenomena. The competition is particularly severe in the case of ferromagnetic order, since both the magnetic ordering and the superconductivity are $q=0$ phenomena. For antiferromagnetic order the peak in the susceptibility appears at, or near, the zone boundary and the two ground states can, in principle, coexist microscopically.

Recently, interest in this topic has been reawakened by the discovery of a new class of magnetic superconductors, RNi_2B_2C.[4,5] These are layered intermetallic compounds with superconducting transition temperatures, T_C as high as $T_C=16.6$ K (for $R=$Lu), which decrease with increasing de Gennes factor, $(g-1)^2J(J+1)$, and Néel temperatures as high as $T_N=10.3$ K (for $R=$Dy), which scale directly with the deGennes factor. Band-structure calculations suggest that the superconductivity is ''conventional'',[6–9] which would put these materials amongst those conventional BCS superconductors with the highest T_C's. The antiferromagnetism is characterized by a rich variety of phases among the different members of the series, including simply commensurate (C) and incommensurate (IC) structures.

In this work, we focus on the magnetic phase behavior of one member of the series, $HoNi_2B_2C$ ($T_C=8.5$ K, $T_N\approx7$ K). This compound is particularly interesting because it exhibits a large reduction, or extinction, of the superconducting order parameter[10–12] in the incommensurate antiferromagnetic phase. The low-temperature commensurate spin structure is well understood and consists of moments aligned ferromagnetically within the a-b planes. These ferromagnetic sheets are stacked in alternating directions along the c axis.[13,14] The ordered moment is $8.7\mu_B$.[14] In terms of the competition with the superconductivity, the incommensurate phase is more interesting, though determining the spin structure has proven problematic.[13,14] Here, we present a detailed study of the incommensurate modulations. Our data allow a simplification of the phenomenology of these structures and we discuss the implications for the competition with the superconducting condensate.

We have chosen to investigate the antiferromagnetic order using the technique of x-ray magnetic scattering, complemented by high-resolution magnetic neutron diffraction. This approach has a number of advantages. First, the reciprocal space resolution achievable with x rays is an order of magnitude better than commonly obtained with neutron diffraction, greatly facilitating the investigation of large length scale magnetic phenomena. Second, the polarization dependences of the x-ray and neutron-scattering cross sections are different and therefore the techniques provide a useful complement to one another in determining spin structures. Third, resonant x-ray magnetic scattering is element specific and therefore can separate (in this case) the Ho ordered moment from that of the Ni. Each of these advantages plays a role in this study, revealing an incommensurate antiferromagnetic state that is considerably more complex than was previously realized.

$HoNi_2B_2C$ forms a tetragonal structure with lattice constants $a=3.51$ Å and $c=10.53$ Å at $T=2$ K. The unit cell consists of two Ho-C layers separated by a Ni_2B_2 complex.[15] The superconductivity is believed to originate in the Ni_2B_2 layers. On cooling through the transition at $T_C=8$ K the superconducting order parameter is seen to increase, as measured by the upper critical field (H_{C2}),[10,13,12] until $T_N\approx7$ K when it decreases, coincident with the appearance of the IC satellites. In earlier studies, two ordering wave vectors were reported, $\mathbf{q}_c=0.915\mathbf{c}^*$ (Refs. 13 and 14) and $\mathbf{q}_a=0.585\mathbf{a}^*$.[13] A third harmonic of the c-axis modulation indicates that it is not perfectly sinusoidal.[13] At $T_{\text{IC-C}}=5$ K, a first-order transition into the commensurate phase is observed.

Resonant x-ray magnetic scattering utilizes atomic absorption edges to obtain large enhancements in the magnetic scattering cross section.[16,17] The enhancements are largest

when there is a substantial overlap between the initial and excited wave functions. Here, we find the Ho L_{III} edge provides the strongest signal and the x-ray scattering data presented below were taken at this energy. The dipole terms (i.e., $2p_{3/2} \rightarrow 5d$), are expected to be dominant so that the technique is sensitive to the polarization of the $5d$ bands induced by the localized Ho $4f$ moments.

Single crystals of $HoNi_2B_2C$ were grown at Ames Laboratory using the high-temperature flux technique.[11,18] For the x-ray work, a platelet of size $4\times4\times0.5\times$ mm^3 was used with a mosaic of 0.03° half width half maximum (HWHM), as measured by x-ray scattering. A surface, normal to the c axis, was prepared by mechanical polishing followed by annealing at 900 °C in high vacuum. The sample was wrapped in aluminum foil to eliminate local heating effects,[19] and mounted at the end of the cold finger of a closed-cycle He cryostat in He exchange gas. A sample from the same batch was used for the neutron work, and mounted similarly. The mosaic spread of this sample was resolution limited, as determined by neutron diffraction, that is less than 0.1° (HWHM).

The x-ray experiments were performed at beamline X22C at the National Synchrotron Light Source. This beamline is equipped with a toroidal focusing mirror for harmonic rejection and a double bounce Ge(111) monochromator. A Ge(111) analyzer was employed to provide a longitudinal resolution of 6×10^{-4} Å^{-1} (HWHM) at the (003) position. The scattering plane was vertical, that is perpendicular to the plane of the electron orbit and therefore perpendicular to the incident photon polarization. The transverse resolution was dominated by the sample mosaic. The out-of-plane resolution was controlled by collimating slits and was $\approx$0.01 Å^{-1} HWHM. The neutron-scattering data reported here were taken on the H9 spectrometer at the High Flux Beam Reactor operating at an incident energy $E_i=3.5$ meV. The collimation was set to 60-40-15-S-5-10, resulting in a longitudinal resolution of 0.004 Å^{-1} (HWHM). A pyrolytic graphite (002) monochromator and analyzer determined the initial and final energies, respectively. For both the x-ray and neutron work reciprocal-lattice vectors of the form $(h0l)$ were accessible.

The central results of this paper are summarized in Fig. 1, in which x-ray scattering scans taken along the $(00l)$ axis in the vicinity of the (003) antiferromagnetic Bragg peak are shown. At low temperatures (top panel) a single, sharp peak is observed at the (003) position corresponding to a well ordered antiferromagnetic structure. Data analysis, outlined below, shows a c-axis correlation length of $\approx$5300 Å. The bottom panel shows data taken in the IC phase at $T=5.4$ K. The high-resolution of x-ray scattering reveals that the IC c-axis satellite around $\mathbf{Q}=2.915\mathbf{c}^*$ consists of two peaks, one at $\mathbf{q}_1=0.906\mathbf{c}^*$ and the other at $\mathbf{q}_2=0.919\mathbf{c}^*$. In addition, an a-axis satellite with $\mathbf{q}_a=0.585\mathbf{a}^*$ is also observed at these temperatures, in agreement with the neutron-scattering results of Ref. 13. A schematic of reciprocal space is shown in the inset of the top panel of Fig. 1. Here $\delta_1=1-q_1$, etc. To discount the possibility that the splitting is in some way due to the sensitivity of x rays to the near-surface region of the sample, high-resolution neutron diffraction was also performed. These data are shown in the inset to the bottom panel of Fig. 1. The incommensurate satellite is again seen to be split, confirming that this behavior is representative of the bulk. In the x-ray data, the satellite peak at $2+q_1$ is extremely sharp, implying that this ordering extends over regions well in excess of 5000 Å in size. To extract estimates of correlation lengths, the $2+q_1$ peak was taken to be resolution limited and fitted to a Lorentzian squared line shape. To analyze other c-axis data we then convolved this line shape with a Lorentzian signal function in a one-dimensional integral. In the IC phase, the (003) peak and $2+q_2$ satellite are both broadened, indicating the presence of disorder in these structures.

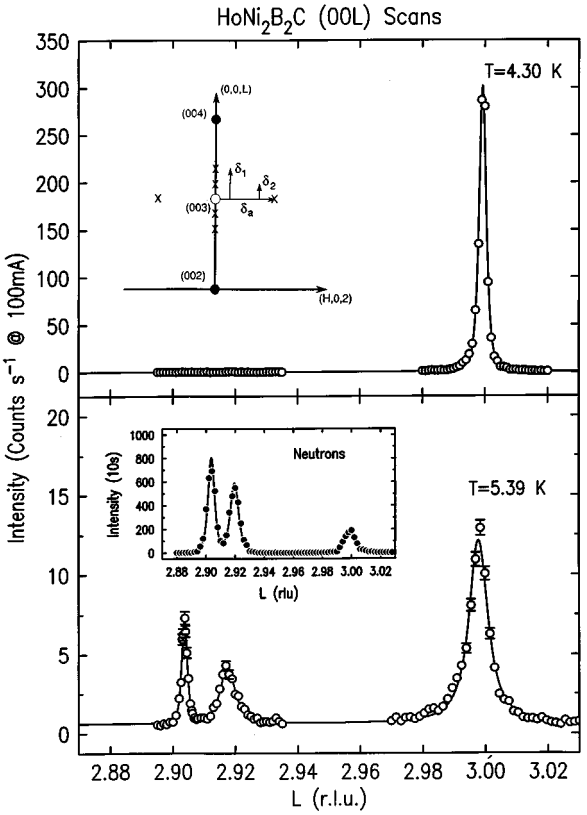

FIG. 1. Longitudinal x-ray scans in the vicinity of the (003) antiferromagnetic reciprocal-lattice point. These data were taken with the incident photon energy tuned to the Ho L_{III} edge. (Top) $T=4.3$ K. Only the commensurate peak is present. Inset. Schematic of reciprocal space. Closed (open) circles represent charge (antiferromagnetic) Bragg peaks. The crosses correspond to the incommensurate satellites present for temperatures above $T=5.2$ K. Higher-order incommensurate peaks are not shown. (Bottom) Data taken at $T=5.39$ K, in the incommensurate phase. The IC peak is comprised of two satellites at $(0,0,2+q_1)$ and $(0,0,2+q_2)$. The (003) commensurate peak is still present but significantly reduced and broadened. Inset. High-resolution neutron-scattering data taken at an equivalent temperature confirming that the splitting of the IC satellite is a bulk effect.

The temperature dependence of the (003) magnetic peak intensity is shown in Fig. 2(a). At low temperatures the intensity is approximately constant, suggestive of a saturated order parameter. At $T=5.2$ K, the intensity abruptly falls. This coincides with the appearance of incommensurate satellite peaks, and marks the first-order C-IC transition. The (003) intensity decays more slowly as the temperature is increased further. The deconvolved width of the Lorentzian fit is plotted in Fig. 2(b). Below the transition it is almost resolution limited. Above $T=5.2$ K the peak broadens, reach-

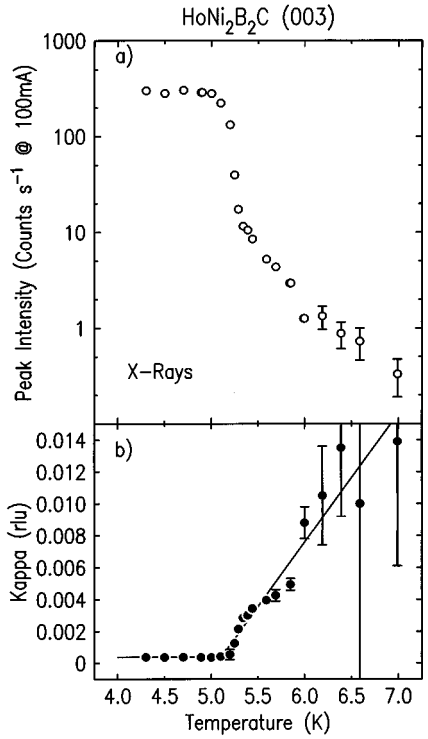

FIG. 2. Temperature dependence of the (003) commensurate antiferromagnetic Bragg peak. (a) The peak intensity. (b) The deconvolved width (see text), κ of a Lorentzian line shape. The solid line is a guide to the eye.

ing a correlation length of $\xi_c = 500$ Å at $T = 5.44$ K. Our inelastic neutron-scattering data suggest that the broadening is not due to dynamic fluctuations, but to static or quasistatic disorder. Interestingly, the size of these commensurate regions is approximately the same as the incommensurate domains discussed below.

The peak intensities of the three incommensurate satellites are plotted in Fig. 3(a). No incommensurate scattering is observed below $T = 5.2$ K. Above this temperature the incommensurate satellites abruptly appear with relatively large intensities. As the temperature is raised, all three satellites exhibit similar behaviors, peaking at, or near, $T = 5.3$ K before decreasing slowly. Above $T = 5.5$ K only one c-axis satellite, in addition to the a-axis satellite, can be resolved. Consequently a single Lorentzian signal function is used and these data are plotted as shaded symbols. We emphasize that these data were taken at the Ho L_{III} edge and therefore the observation of both the a- and c-axis satellites is strong evidence that the Ho moments participate in both modulations.

The widths of the IC satellites are plotted in Fig. 3(b). The c-axis peak widths were obtained using the deconvolution procedure outlined above. However, the a-axis satellite width is dominated by sample mosaic and these data were not deconvolved. There is no observable change in this width, to within errors. The temperature dependence of the δ_1 and δ_2 satellite widths is intriguing. δ_1 remains resolution limited at all temperatures for which it may be resolved, indicative of an extremely well-ordered structure. Indeed there is some evidence that it is more highly ordered than the low-temperature commensurate structure [perhaps reflecting a coupling of the commensurate order parameter in

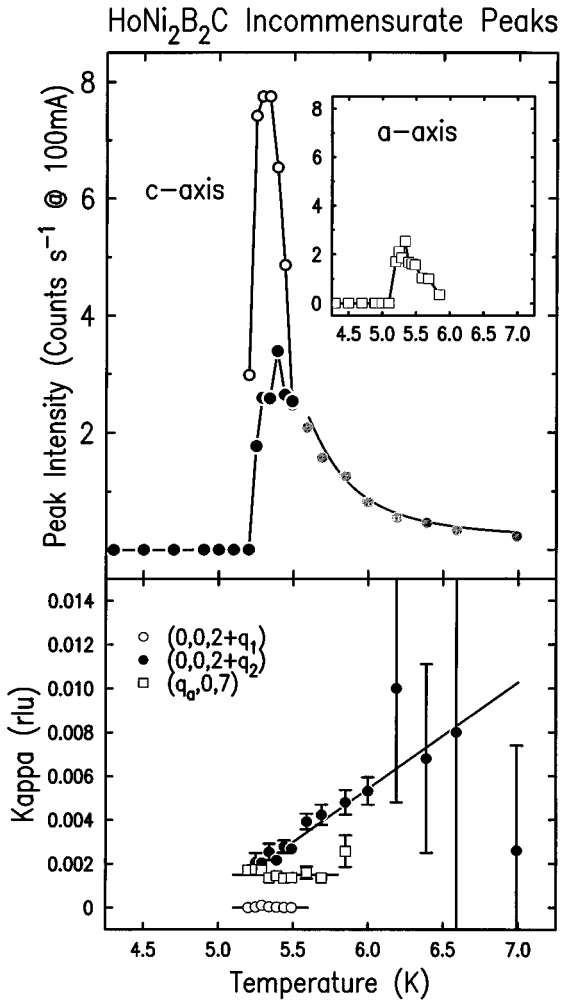

FIG. 3. Temperature dependence of the incommensurate satellites. (Top) Peak intensities. The open (closed) circles represent the $\mathbf{q}_1$ ($\mathbf{q}_2$) satellites. The shaded circles represent data for which the two could not be resolved and were consequently fit to a single peak. The open squares represent the peak intensity of the a-axis satellite as measured at ($\mathbf{q}_a$,0,7). (Bottom) The widths, κ of Lorentzian fits to the c-axis satellites. The a-axis satellites widths are the result of Lorentzian-squared fits.

$HoNi_2B_2C$ to random strains in the sample, as has been observed for the spiral order parameter in pure Ho (Ref. 20)]. The δ_2 modulation is disordered with a correlation length similar to the (003) domains at similar temperatures, e.g., $\xi_c(\delta_2) = 600$ Å at $T = 5.44$ K.

In Fig. 4, the modulation wave vectors, δ_1, δ_2, and δ_a are plotted as a function of temperature. The c-axis modulations were calculated with respect to the (004) Bragg peak position, which remains fixed over this temperature range; the thermal expansion of the c-axis lattice constant is minimal and was ignored in this analysis. The a-axis modulation, δ_a, is plotted in units of a^* and again thermal expansion is assumed negligible. We find all three modulations to be temperature dependent. (Interestingly, in the temperature region in which both δ_1 and δ_2 are resolved, there is a linear relationship between the two; the change in δ_2 is five times that of δ_1, a result also seen in our high-resolution neutron data. The significance of this correlation is not clear.) At high tem-

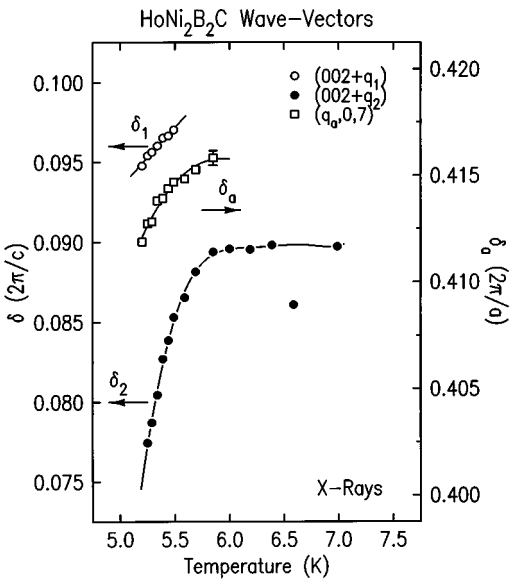

FIG. 4. Temperature dependence of the incommensurate wave vectors. The c-axis satellite wave vectors δ_1 and δ_2 (open and closed circles, respectively) are referred to the left-hand scale. The open squares represent the a-axis satellite position and have not been corrected for any expansion of the lattice. They are referred to the right-hand scale. Note the y-axis scale size is identical for left- and right-hand axes.

peratures the c-axis modulation wave vector appears to lock-in to a value close to 0.09.

We now turn to a discussion of the spin structure in the incommensurate phase. This is seemingly complex, with four independent wave vectors to account for. However, our data allow some simplification.

First, the scattering that is the apparent remnant of the (003) commensurate peak is in fact no longer commensurate with the average bulk lattice, but shifts to progressively smaller l as the temperature is raised. In addition, the peak becomes weaker and broader. Similar behavior was observed in the x-ray magnetic scattering near the first-order antiferromagnetic transition of UO_2.[21] In this case, the effect of near-surface strains nucleating finite-sized ordered domains was considered to explain the shift and broadening observed above T_N, the so-called ''two-length scale problem.'' A similar explanation may apply here. A surface bias to the location of such strains would explain the relatively weak (003) intensity in the neutron data.[22] In this picture, the remnant commensurate scattering arises from domains of the low-temperature phase and does not coexist microscopically with the IC modulations, that is the IC domains do not simultaneously support the commensurate remnants.

The next question to address is whether the c- and a-axis modulations correspond to distinct domains, or if they form a double-**Q** structure. An extensive search was carried out for third harmonic satellites of the form $2\mathbf{q_c}+\mathbf{q_a}$ or $2\mathbf{q_a}+\mathbf{q_c}$, using neutron diffraction. These can only be present if the modulations arise from a single spin structure. No such peaks were observed, leading to an upper bound on their intensity of 2×10^{-4} of the fundamental. In contrast, the intensity of the $3\delta_c$ peak is 3×10^{-2} of the fundamental. We also find that the phase behaviors of the two modulations are different in a b-axis applied field. We, therefore, tentatively conclude that the a-axis and c-axis modulations correspond to separate domains.

One is now left with two distinct IC spin structures to describe. Taking the a-axis modulation first, we note that modulations of similar wave vector have been observed in the Er ($\delta_a=0.553a^*$) (Refs. 23 and 24) and Gd ($\delta_a=0.553a^*$) (Ref. 25) members of the series. Both compounds form transversely polarized sinusoidal modulations. The similarity of the wave vectors in the three materials, together with band-structure calculations[26] which show a peak in the susceptibility near $\mathbf{Q}=0.6\mathbf{a}^*$ in $LuNi_2B_2C$, due to a nesting of the Fermi surface, suggest a common origin to this modulation. In $HoNi_2B_2C$, the apparent coexistence of the a- and c-axis modulations implies that the two structures have closely similar free energies. In such a situation, regions of each phase may be stabilized by, e.g., strain, lattice defects or impurities. Given the large correlation length observed in the x-ray experiments, these regions must be relatively large in agreement with previous single-crystal neutron-scattering measurements. The influence of strain may help explain some of the discrepancies between the single crystal and powder neutron work.[13,14]

The complementarity of the x-ray and neutron-scattering data provide constraints on the structure of the a-axis modulation. The neutron cross section is sensitive to the components of the moment perpendicular to the momentum transfer, hence the presence of the $(\delta_a,0,0)$ satellite requires a transverse ordered moment. At the same time, the resonant cross section[27] requires an ordered moment in the a-c plane to produce the observed $(1-\delta_a,0,7)$ satellite. These observations, together with magnetization measurements which imply that the moments lie in the basal plane,[11] suggest the existence of a longitudinal component (i.e., along $\mathbf{a}^*$) as well as the transverse component ($\mathbf{b}^*$) seen in Er and Gd.[25] Depending on the relative phase of the two components, the resulting structure is either an in-plane spiral, or a linear modulation with the moments at a fixed angle to the b axis.

The c-axis structure consists of a well ordered incommensurate structure together with a disordered structure of slightly different wavelength. Both neutron (see also Refs. 13 and 14) and x-ray polarization dependences are consistent with a basal plane spiral, with a temperature-dependent turn angle of $\approx163°$ per layer.

As mentioned in the introduction, the incommensurate phase coincides with a deep suppression of H_{C2}. Such a suppression, although not common, has been seen before near antiferromagnetic transitions of some RMo_6S_8 compounds[28] and cannot be explained in terms of the multiple pair-breaking theory of Fulde and Maki.[29] An additional pair-breaking mechanism has been postulated[28] which appears to scale like the antiferromagnetic order parameter. Such a mechanism may be in effect here, perhaps associated with the incommensurate order parameter.[12,13,11,18] Alternatively, it is possible that the origin of the dip lies in the incommensurate modulations. Previously, IC structures have been associated with the competition between superconductivity and ferromagnetism. However, this is not the case in RNi_2B_2C, as the presence of such modulations in nonsuperconducting members of the series demonstrates. If this state is responsible for the reduction in H_{C2}, then it may be con-

nected with the Fermi-surface nesting mentioned above. Indeed, pair-breaking mechanisms based on nesting properties do exist.[30,31] A caveat to such speculations, however, is the richness of the temperature and magnetic-field phase diagram[12] which suggests that the energy balance between the numerous competing ground states is quite delicate. Subtle details in the Fermi surface, or even lattice defects may then be important and may result in changes in the electronic structure. This would preclude qualitative arguments and detailed calculations specific to $HoNi_2B_2C$ may be required.

In summary, we have performed high-resolution x-ray and neutron-scattering studies of the antiferromagnetism of $HoNi_2B_2C$. We find that the incommensurate state consists of a number of coexisting phases. These include, an in-plane modulation with propagation vector along the *a* axis, which shares some common features with the low-temperature structures of $ErNi_2B_2C$ and $GdNi_2B_2C$; a *c*-axis basal plane spiral-like structure, which is revealed to consist of two wave vectors, one of which is highly ordered; and some residual short-range-ordered, static, commensurate regions, perhaps resulting from strain. The close interplay between the C and IC antiferromagnetic states and the superconductivity remain to be understood, even qualitatively, and should provide an interesting test case for theories of antiferromagnetic superconductors.

It is a pleasure to acknowledge stimulating conversations with B. N. Harmon. The work at Brookhaven National Laboratory was supported by the Department of Energy, Division of Materials Sciences under Contract No. DE-AC02-76CH00016. Ames Laboratory is operated for the DOE by Iowa State University under Contract No. W-7405-ENG-82.

[1] A. A. Abrikosov and L. P. Gor'kov, Zh. Eksp. Teor. Fiz. **39**, 1781 (1961).
[2] M. B. Maple and O. Fischer, *Superconductivity in Ternary Compounds III* (Springer-Verlag, Berlin, 1982), and references therein.
[3] B. D. Gaulin, D. Gibbs, E. D. Isaacs, J. G. Lussier, J. N. Reimers, A. Schroder, L. Taillefer, and P. Zschack, Phys. Rev. Lett. **73**, 890 (1994), and references therein.
[4] R. Nagarajan *et al.*, Phys. Rev. Lett. **72**, 274 (1994).
[5] R. J. Cava *et al.*, Nature (London) **367**, 252 (1994).
[6] W. E. Pickett and D. J. Singh, Phys. Rev. Lett. **72**, 3702 (1994).
[7] L. F. Mattheiss, Phys. Rev. B **49**, 13 279 (1994).
[8] R. Coehoorn, Physica C **228**, 5671 (1994).
[9] L. F. Mattheiss, T. Siegrist, and R. J. Cava, Solid State Commun. **91**, 587 (1994).
[10] H. Eisaki, Phys. Rev. B **50**, 647 (1994).
[11] P. C. Canfield, B. K. Cho, D. C. Johnston, D. K. Finnemore, and M. F. Hundley, Physica C **230**, 397 (1994).
[12] K. D. D. Rathnayaka, D. G. Naugle, B. K. Cho, and P. C. Canfield, Phys. Rev. B (to be published).
[13] A. I. Goldman *et al.*, Phys. Rev. B **50**, 9668 (1994).
[14] T. E. Grigereit *et al.*, Phys. Rev. Lett. **73**, 2756 (1994).
[15] T. E. Siegrist, H. W. Zandbergen, R. J. Cava, J. J. Krajewski, and W. J. Peck, Jr., Nature (London) **367**, 254 (1994).
[16] D. Gibbs, D. R. Harshmann, E. D. Isaacs, D. B. McWhan, D. Mills, and C. Vettier, Phys. Rev. Lett. **61**, 1241 (1988).
[17] J. P. Hannon, G. T. Trammel, M. Blume, and D. Gibbs, Phys. Rev. Lett. **61**, 1245 (1988).
[18] B. K. Cho, P. C. Canfield, L. L. Miller, D. C. Johnston, W. P. Beyermann, and A. Yatskar, Phys. Rev. B **53**, 3684 (1995).
[19] Without such precautions, beam heating was sufficient to drive the sample from the commensurate phase into the incommensurate phase, a temperature rise of $\approx$2 K.
[20] G. Helgesen, J. P. Hill, T. R. Thurston, D. Gibbs, J. Kwo, and M. Hong, Phys. Rev. B **50**, 2990 (1994).
[21] G. M. Watson, B. D. Gaulin, D. Gibbs, G. H. Lander, T. R. Thurston, P. J. Simpson, and H. J. Matzke, Phys. Rev. B (to be published).
[22] The neutron (003) intensity contains contributions from both the *a* and *b* domains, whereas the x rays are mostly sensitive to the *a* domain.
[23] S. K. Sinha, J. W. Lynn, T. E. Grigereit, Z. Hossain, L. C. Gupta, R. Nagarajan, and C. Godart, Phys. Rev. B **51**, 681 (1995).
[24] J. Zarestsky, C. Stassis, A. I. Goldman, P. C. Canfield, P. Dervenagas, B. K. Cho, and D. C. Johnston, Phys. Rev. B **51**, 678 (1995).
[25] C. Detlefs, A. I. Goldman, J. P. Hill, D. Gibbs, C. Stassis, P. C. Canfield, and B. K. Cho, Phys. Rev. B (to be published).
[26] J. Y. Rhee, X. Wang, and B. N. Harmon, Phys. Rev. B **51**, 15 585 (1995).
[27] J. P. Hill and D. F. McMorrow, Acta Crystallogr. A (to be published).
[28] O. Fischer, in *Ferromagnetic Materials*, edited by K. H. J. Buschow and E. P. Wohlfarth (North-Holland, Amsterdam, 1990), Vol. 5, Chap 6.
[29] P. Fulde and K. Maki, Phys. Rev. **141**, 275 (1966).
[30] T. V. Ramakrishnan and C. M. Varma, Phys. Rev. B **24**, 137 (1981).
[31] K. Machida, K. Nohura, and T. Masubara, Phys. Rev. Lett. **42**, 918 (1980).